Adaptive frequency-domain equalization in digital coherent optical receivers

Md. Saifuddin Faruk* **and Kazuro Kikuchi**

Department of Electrical Engineering and Information Systems, The University of Tokyo, 7-3-1 Hongo, Bunkyo-ku, Tokyo 113-8656, Japan
**faruk@ginjo.t.u-tokyo.ac.jp*

Abstract: We propose a novel frequency-domain adaptive equalizer in digital coherent optical receivers, which can reduce computational complexity of the conventional time-domain adaptive equalizer based on finite-impulse-response (FIR) filters. The proposed equalizer can operate on the input sequence sampled by free-running analog-to-digital converters (ADCs) at the rate of two samples per symbol; therefore, the arbitrary initial sampling phase of ADCs can be adjusted so that the best symbol-spaced sequence is produced. The equalizer can also be configured in the butterfly structure, which enables demultiplexing of polarization tributaries apart from equalization of linear transmission impairments. The performance of the proposed equalization scheme is verified by 40-Gbits/s dual-polarization quadrature phase-shift keying (QPSK) transmission experiments.

OCIS codes: (060.2330) Fiber optic communications; (060.1660) Coherent communications; (060.2920) Homodyning.

References and links

1. K. Kikuchi, "Phase-diversity homodyne detection of multilevel optical modulation with digital carrier phase estimation," IEEE J. Sel. Top. Quantum Electron. **12**(4), 563–570 (2006).
2. K. Kikuchi, "Coherent optical communications: historical perspectives and future directions," in *High Spectral Density Optical Communication Technology*, M. Nakazawa, K. Kikuchi, and T. Miyazaki, eds (Springer, 2010), Chap. 2.
3. C. R. S. Fludger, T. Duthel, D. van den Borne, C. Schulien, E.-D. Schmidt, T. Wuth, J. Geyer, E. De Man, Khoe Giok-Djan, and H. de Waardt, "Coherent equalization and POLMUX-RZ-DQPSK for robust 100-GE transmission," J. Lightwave Technol. **26**(1), 64–72 (2008).
4. S. J. Savory, "Digital filters for coherent optical receivers," Opt. Express **16**(2), 804–817 (2008).
5. K. Kikuchi, "Clock recovering characteristics of adaptive finite-impulse-response filters in digital coherent optical receivers," Opt. Express **19**(6), 5611–5619 (2011).
6. K. Roberts, M. O'Sullivan, Kuang-Tsan Wu, Han Sun, A. Awadalla, D. J. Krause, and C. Laperle, "Performance of dual-polarization QPSK for optical transport system," J. Lightwave Technol. **27**(16), 3546–3559 (2009).
7. B. Spinnler, "Equalizer design and complexity for digital coherent receivers," IEEE J. Sel. Top. Quantum Electron. **16**(5), 1180–1192 (2010).
8. J. Leibrich and W. Rosenkranz, "Frequency domain equalization with minimum complexity in coherent optical transmission systems," in *Optical Fiber Communication Conference*, OSA Technical Digest (Optical Society of America, 2010), paper OWV1.
9. M. Selmi, P. Ciblat, Y. Jaouen, and C. Gosset, "Block versus adaptive MIMO equalization for coherent PolMux QAM transmission system," in *Proceedings of European Conference on Optical Communication* (2010), paper Th.9.A.5.
10. J. C. Geyer, C. R. S. Fludger, T. Duthel, C. Schulien, and B. Schmauss, "Efficient frequency domain chromatic dispersion compensation in a coherent polmux QPSK-receiver," in *Optical Fiber Communication Conference*, OSA Technical Digest (Optical Society of America, 2010), paper OWV5.
11. R. Kudo, T. Kobayashi, K. Ishihara, Y. Takatori, A. Sano, and Y. Miyamoto, "Coherent optical single carrier transmission using overlap frequency domain equalization for long-haul optical systems," J. Lightwave Technol. **27**(16), 3721–3728 (2009).
12. M. Kuschnerov, F. N. Hauske, K. Piyawanno, B. Spinnler, A. Napoli, and B. Lankl, "Adaptive chromatic dispersion equalization for non-dispersion managed coherent systems," in *Optical Fiber Communication Conference*, OSA Technical Digest (Optical Society of America, 2009), paper OMT1.
13. R. Kudo, T. Kobayashi, K. Ishihara, Y. Takatori, A. Sano, E. Yamada, H. Masuda, and Y. Miyamoto, "PMD compensation in optical coherent single carrier transmission using frequency-domain equalization," Electron. Lett. **45**(2), 124–125 (2009).

#145673 - $15.00 USD Received 11 Apr 2011; revised 20 May 2011; accepted 10 Jun 2011; published 17 Jun 2011

14. K. Ishihara, T. Kobayashi, R. Kudo, Y. Takatori, A. Sano, and Y. Miyamoto, "Frequency-domain equalization for coherent optical single-carrier transmission systems," IEICE Trans. Commun. **E92-B**(12), 3736–3743 (2009).
15. J. J. Shynk, "Frequency-domain and multirate adaptive filtering," IEEE Signal Process. Mag. **9**(1), 14–37 (1992).
16. S. Haykin, *Adaptive Filter Theory*, 3rd ed., (Prentice Hall, 2001).
17. Md. S. Faruk, Y. Mori, C. Zhang, and K. Kikuchi, "Proper polarization demultiplexing in coherent optical receiver using constant modulus algorithm with training mode," in *Proceedings of Optoelectronics and Communication Conference* (2010), paper 9B3–3.
18. D.-S. Ly-Gagnon, S. Tsukamoto, K. Katoh, and K. Kikuchi, "Coherent detection of optical quadrature phase-shift keying signals with carrier phase estimation," J. Lightwave Technol. **24**(1), 12–21 (2006).

1. Introduction

The next-generation optical network is going to employ digital coherent optical receivers, which enable high spectral efficiency by the use of multi-level optical modulation formats, dense wavelength-division multiplexing, and polarization multiplexing [1,2]. Moreover, those receivers allow compensation for linear transmission impairments such as group-velocity dispersion (GVD) and polarization-mode dispersion (PMD), by using adaptive equalization in the electrical domain [3,4].

Key issues in digital coherent receivers are analog-to-digital conversion of the received sequence and succeeding digital signal processing (DSP). First, the received sequence is sampled by free-running analog-to-digital converters (ADCs) operated at the rate twice the symbol rate (*i.e.*, twofold oversampling). Such oversampling significantly reduces the aliasing effect. Next, we use time-domain finite-impulse-response (FIR) filters in the butterfly structure, where filter-tap weights are adapted every two samples through the constant-modulus algorithm (CMA). With such a time-domain equalizer (TDE), we can achieve the following three functions simultaneously: (1) Linear impairments stemming from GVD and tight optical/electrical filtering are adaptively equalized. (2) We can demultiplex polarization tributaries and compensate for PMD. (3) The initial sampling phase, which has been decided by free-running ADC, is adjusted optimally during the filter-tap adaptation process, as far as clock frequencies are synchronized between the transmitter and the receiver. This is because the sampled waveform is continuously time-shifted so that sampling instance for the symbol-spaced sequence comes to the best positions in symbol duration. Such function is essentially clock recovery, and details of clock-recovery characteristics by adaptive FIR filters can be found in [5].

Computational complexity of FIR filters, however, increases with the number of delay taps; therefore, it becomes difficult to implement FIR filters having a large number of delay taps in the application-specific integrated circuit (ASIC) or the field-programmable gate array (FPGA) due to large power consumption and high gate density [6]. On the other hand, frequency-domain equalization can reduce this computational cost by block-by-block signal processing and efficient implementation of discrete Fourier transform (DFT) [7,8]. Such block processing is applicable to optical communication system because propagation-channel parameters vary much more slowly than the block rate [9].

Recently, several reports on the frequency-domain equalizer (FDE) for coherent optical receivers have been presented [10–14]. In [10] and [11], only a fixed amount of GVD of fibers for transmission was compensated for with FDE, while adaptive equalization was left in the time-domain. The adaptive FDE for GVD was proposed in [12], where a look-up table was employed to update tap weights of the equalizer; however, such a complex equalizer failed to compensate for any polarization-related impairment. Although in [13] and [14], the adaptive FDE was realized by estimating the channel transfer function by using the cyclic prefix and the pilot-symbol sequence, such an approach generally decreases the spectral efficiency of transmission systems.

On the other hand, in this paper, we propose a fully-adaptive FDE, which maintains all the advantages of the adaptive FIR-filter-based TDE. Even in the block processing environment of FDE, it can work on the twofold-oversampled input sequence by introducing even and odd sub-equalizers; consequently, we can achieve adaptive equalization together with polarization demultiplexing and sampling-phase adjustment, using the CMA-based tap-adaptation algorithm. The principle of operation of the proposed equalizer is verified by dual-polarization

#145673 - $15.00 USD Received 11 Apr 2011; revised 20 May 2011; accepted 10 Jun 2011; published 17 Jun 2011

quadrature phase-shift keying (QPSK) transmission experiments with mixed channel distortions stemming from GVD, the first-order PMD, and polarization-dependent loss (PDL). The bit-error-rate (BER) performance is similar to that obtained by the conventional FIR-filter-based TDE; however, the proposed FDE can be implemented with reduced computational complexity.

The rest of the paper is organized as follows: Section 2 discusses the principle of operation of our proposed FDE. In Sec. 3, computational complexity of the proposed FDE is analyzed and compared with that of the conventional TDE. Section 4 provides experimental verifications of the proposed scheme, and finally Sec. 5 concludes our paper.

Throughout the remainder, time- and frequency-domain variables are denoted by lower- and upper-case characters, respectively, while boldface characters denote vectors. Furthermore, the symbol $*$ represents convolution and $\otimes$ element-by-element multiplication; $\mathbf{O}_{\mathrm{L}}$ is a column vector with L zeros; superscripts $(\bullet)^e$ and $(\bullet)^o$ correspond to even and odd sub-equalizer parameters, respectively; and conj(•) is the conjugate operator.

2. Proposal of a novel frequency-domain equalizer

2.1 Equivalence of the half-symbol-spaced FIR filter with even and odd sub-equalizers

We define input ports of the two-by-two butterfly-structured FIR filters as *x* and *y* ports, whereas their output ports as *X* and *Y* ports. The symbol duration is *T*, the delay spacing is *T*/2, and the delay-tap length of each filter is *N*. When $u_x(n)$ and $u_y(n)$ are *n*-th input sequences for *x* and *y* ports, respectively, which are twofold oversampled, the output from the *X* port can be expressed as

$$v_x(n) = \sum_{i=0}^{N-1} h_{xx_i}(n) u_x\left\{(n-i)\frac{T}{2}\right\} + \sum_{i=0}^{N-1} h_{xy_i}(n) u_y\left\{(n-i)\frac{T}{2}\right\}. \tag{1}$$

Filter-tap weights are updated every two samples, and the filter output is down-sampled by a factor of two to retain the symbol-spaced output. Without loss of generality, we consider that only the odd sequence from the output is taken and used for updating filter-tap weights. Let the new symbol-spaced sample index be *m* such that $n = 2m+1$ (m = 0, 1, 2, ⋯); and then, the down-sampled output from the *X* port can be written as

$$\begin{aligned}
v_x(m) &= \sum_{i=0}^{N-1} h_{xx_i}(m) u_x\left\{(2m+1-i)\frac{T}{2}\right\} + \sum_{i=0}^{N-1} h_{xy_i}(m) u_y\left\{(2m+1-i)\frac{T}{2}\right\} \\
&= \sum_{i=0}^{N-1} h_{xx_i}(m) u_x\left\{\left(mT - i\frac{T}{2}\right) + \frac{T}{2}\right\} + \sum_{i=0}^{N-1} h_{xy_i}(m) u_y\left\{\left(mT - i\frac{T}{2}\right) + \frac{T}{2}\right\} \\
&= \sum_{i=0}^{N/2-1} h_{xx_{2i}}(m) u_x\left\{\left(mT - 2i\frac{T}{2}\right) + \frac{T}{2}\right\} + \sum_{i=0}^{N/2-1} h_{xy_{2i}}(m) u_y\left\{\left(mT - 2i\frac{T}{2}\right) + \frac{T}{2}\right\} \\
&\quad + \sum_{i=0}^{N/2-1} h_{xx_{2i+1}}(m) u_x\left\{\left(mT - (2i+1)\frac{T}{2}\right) + \frac{T}{2}\right\} + \sum_{i=0}^{N/2-1} h_{xy_{2i+1}}(m) u_y\left\{\left(mT - (2i+1)\frac{T}{2}\right) + \frac{T}{2}\right\} \\
&= \sum_{i=0}^{N/2-1} h_{xx_{2i}}(m) u_x\left\{(m-i)T + \frac{T}{2}\right\} + \sum_{i=0}^{N/2-1} h_{xy_{2i}}(m) u_y\left\{(m-i)T + \frac{T}{2}\right\} \\
&\quad + \sum_{i=0}^{N/2-1} h_{xx_{2i+1}}(m) u_x\left\{(m-i)T + T\right\} + \sum_{i=0}^{N/2-1} h_{xy_{2i+1}}(m) u_y\left\{(m-i)T + T\right\}.
\end{aligned} \tag{2}$$

We consider that *N* is even so that $L = N/2$ is an integer for the sake of derivational simplicity. Equation (2) shows that the down-sampled output is the sum of two symbol-spaced convolutions with a relative delay of *T*/2. Thus, Eq. (2) can be rewritten as

#145673 - $15.00 USD Received 11 Apr 2011; revised 20 May 2011; accepted 10 Jun 2011; published 17 Jun 2011

$$v_x(m) = \mathbf{h}_{xx}^{e}(m) * \mathbf{u}_x^{e}(m) + \mathbf{h}_{xy}^{e}(m) * \mathbf{u}_y^{e}(m) + \mathbf{h}_{xx}^{o}(m) * \mathbf{u}_x^{o}(m) + \mathbf{h}_{xy}^{o}(m) * \mathbf{u}_y^{o}(m) \ , \quad (3)$$

and similarly, the output from the *Y* port can be written as

$$v_y(m) = \mathbf{h}_{yx}^{e}(m) * \mathbf{u}_x^{e}(m) + \mathbf{h}_{yy}^{e}(m) * \mathbf{u}_y^{e}(m) + \mathbf{h}_{yx}^{o}(m) * \mathbf{u}_x^{o}(m) + \mathbf{h}_{yy}^{o}(m) * \mathbf{u}_y^{o}(m) \ , \quad (4)$$

where $\mathbf{u}_{x,y}^{e}(m)$ and $\mathbf{u}_{x,y}^{o}(m)$ are given as

$$\mathbf{u}_{x,y}^{e}(m) = [u_{x,y}(2m), u_{x,y}(2m-2), u_{x,y}(2m-4), \cdots, u_{x,y}(2m-2L)]^{\mathrm{T}} \ , \quad (5)$$

$$\mathbf{u}_{x,y}^{o}(m) = [u_{x,y}(2m+1), u_{x,y}(2m-1), u_{x,y}(2m-3), \cdots, u_{x,y}(2m-2L+1)]^{\mathrm{T}} \ . \quad (6)$$

On the other hand, filter-tap coefficient vectors $\mathbf{h}_{pq}^{e,o}(m)$ are given as

$$\mathbf{h}_{pq}^{e}(m) = [h_{pq_0}(m), h_{pq_2}(m), \cdots h_{pq_{2L-2}}(m)]^{\mathrm{T}}, \quad (7)$$

$$\mathbf{h}_{pq}^{o}(m) = [h_{pq_1}(m), h_{pq_3}(m), \cdots h_{pq_{2L-1}}(m)]^{\mathrm{T}}, \quad (8)$$

where *p* and *q* are either *x* or *y*. Thus, we may split the equalizer into even and odd sub-equalizers with tap coefficients taken from even and odd filter-tap indices. Correspondingly, the input sequences for the sub-equalizers are taken from even and odd samples of twofold-oversampled sequences. Eventually, instead of updating tap coefficients of conventional *T*/2-spaced FIR filters every two samples, we can use even and odd sub-equalizers, where tap updating is done every symbol without down-sampling output sequences.

It should be noted that time-domain adaptive equalizer based on the gradient decent algorithm can be implemented by FDE with less computational complexity. Such adaptive FDE works in the block processing mode, where the symbol-spaced sequence should be included [15]. In case of the symbol-spaced input sequence, we can construct the gradient vector from each output block, whose length is equal to that of the filter-tap coefficient vector. On the other hand, if we use twofold-oversampled input sequences and down-sample the output sequences from each output block, we have an insufficient number of symbol-spaced output samples to construct the gradient vectors. However, splitting the FDE into even and odd sub-equalizers enables each sub-equalizer to operate on symbol-spaced sequences; and thus, the FDE can finally work on twofold-oversampled input sequences.

With such sub-equalizer-based FDE, we can efficiently execute time-domain convolutions shown in Eqs. (3) and (4) in the frequency-domain by using discrete Fourier transform (DFT) and multiplications. Block-output vectors with *L* rows are given as

$$\mathbf{V}_x(k) = \mathbf{H}_{xx}^{e}(k) \otimes \mathbf{U}_x^{e}(k) + \mathbf{H}_{xx}^{o}(k) \otimes \mathbf{U}_x^{o}(k) + \mathbf{H}_{xy}^{e}(k) \otimes \mathbf{U}_y^{e}(k) + \mathbf{H}_{xy}^{o}(k) \otimes \mathbf{U}_y^{o}(k) \ , \quad (9)$$

$$\mathbf{V}_y(k) = \mathbf{H}_{yx}^{e}(k) \otimes \mathbf{U}_x^{e}(k) + \mathbf{H}_{yx}^{o}(k) \otimes \mathbf{U}_x^{o}(k) + \mathbf{H}_{yy}^{e}(k) \otimes \mathbf{U}_y^{e}(k) + \mathbf{H}_{yy}^{o}(k) \otimes \mathbf{U}_y^{o}(k), \quad (10)$$

where *k* is the block index related to the sample index *m* as $m = kL + i$ $(i = 0, 1, \cdots, L-1)$. Note that the convolutions in Eqs. (3) and (4) are linear convolutions, while inverse DFT (IDFT) of Eqs. (9) and (10) gives us circular convolutions. However, using the overlap-save method, we can extract linearly-convoluted terms from the circularly-convoluted terms obtained from IDFT of Eqs. (9) and (10) [15].

2.2 Configuration of the proposed frequency-domain equalizer

The schematic of the proposed adaptive FDE for polarization-multiplexed transmission systems is shown in Fig. 1, which is implemented by using Eqs. (9) and (10). Eight frequency-domain filters consist of even sub-equalizers and odd sub-equalizers. Four even sub-

#145673 - $15.00 USD Received 11 Apr 2011; revised 20 May 2011; accepted 10 Jun 2011; published 17 Jun 2011

equalizers $\mathbf{H}_{xx}^{e}(k), \mathbf{H}_{xy}^{e}(k), \mathbf{H}_{yx}^{e}(k)$, and $\mathbf{H}_{yy}^{e}(k)$ are connected in a two-by-two butterfly configuration. In the same way, four odd sub-equalizers $\mathbf{H}_{xx}^{o}(k)$, $\mathbf{H}_{xy}^{o}(k)$, $\mathbf{H}_{yx}^{o}(k)$, and $\mathbf{H}_{yy}^{o}(k)$ are placed in another two-by-two butterfly configuration.

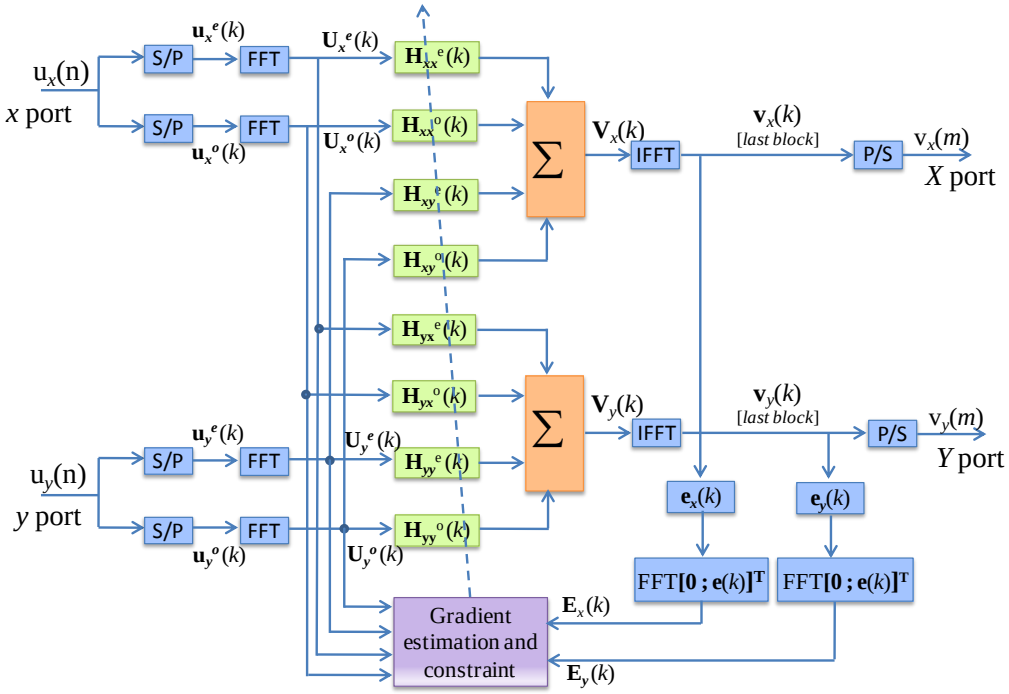

Fig. 1. Schematic of the proposed adaptive FDE. S/P denotes a serial-to-parallel converter and P/S a parallel-to-serial converter.

First, the input sequences $u_{x,y}(n)$ are divided into even and odd sequences. In the FDE, a block of data is processed at a time instead of sample-by-sample processing in the time-domain. Let the length of even and odd sequences included in a block be L. Then, $\mathbf{u}_{x,y}^{e,o}(k)$ represents a column vector with the length of L for the k-th block.

For fast implementation of linear convolution in the frequency-domain, either the overlap-save or the overlap-add method can be employed [15], and we choose the former one for its lower complexity. Moreover, we choose 50% overlap because the most efficient implementation can be achieved with such an overlapping factor [16]. By using the 50% overlapping factor, the frequency-domain input vector $\mathbf{U}_{x,y}^{e,o}(k)$ for sub-equalizers includes L samples from the current block and L samples from the previous block and can be written as

$$\mathbf{U}_{x,y}^{e,o}(k) = \mathrm{FFT}[u_{x,y}^{e,o}(kL-L), \cdots, u_{x,y}^{e,o}(kL+L-1)]^{\mathrm{T}}, \tag{11}$$

where DFT is performed by fast Fourier transform (FFT). Then, L tap weights of the sub-equalizers are padded with the equal number of zeros and $2L$-point FFT is executed. Let $\mathbf{H}_{pq}^{e,o}(k)$ be the FFT-coefficient vector of the zero-padded tap-weight vector $\mathbf{h}_{pq}^{e,o}(k)$ as

$$\mathbf{H}_{pq}^{e,o}(k) = \mathrm{FFT}[\mathbf{h}_{pq}^{e,o}(k); \mathbf{O}_{L}]^{\mathrm{T}}. \tag{12}$$

#145673 - $15.00 USD Received 11 Apr 2011; revised 20 May 2011; accepted 10 Jun 2011; published 17 Jun 2011

By carrying out inverse FFT (IFFT), the output vector in the time-domain with a column length of L is given as

$$\mathbf{v}_{x,y}(k) = \text{last } L \text{ elements of IFFT}\{\mathbf{V}_{x,y}(k)\}, \tag{13}$$

where $\mathbf{V}_x(k)$ and $\mathbf{V}_y(k)$ are given as Eqs. (9) and (10), and the first L elements of IFFT$\{\mathbf{V}_{x,y}(k)\}$ are discarded to implement the linear convolution. Then, the error in CMA is calculated in the time domain and the error vector with the column length of L is given as

$$\mathbf{e}_{x,y}(k) = [\mathbf{I}_L - \mathbf{v}_{x,y}(k) \otimes \text{conj}\{\mathbf{v}_{x,y}(k)\}] \otimes \mathbf{v}_{x,y}(k), \tag{14}$$

where the vector $\mathbf{I}_L$ has L rows and all of its elements are 1. After augmenting $\mathbf{e}_{x,y}(k)$ with L zeros, we convert it to the frequency-domain vector with the column length of $2L$ as

$$\mathbf{E}_{x,y}(k) = \text{FFT}[\mathbf{O}_L; \mathbf{e}_{x,y}(k)]^{\text{T}} . \tag{15}$$

Applying the overlap-save method, we calculate the gradient vector $\nabla_{pq}^{e,o}(k)$ as

$$\nabla_{pq}^{e,o}(k) = \text{first } L \text{ terms of IFFT}[\mathbf{E}_p \otimes \text{conj}\{\mathbf{U}_q^{e,o}(k)\}]^{\text{T}} . \tag{16}$$

Finally, tap weights are updated in the frequency-domain by using the gradient decent algorithm as

$$\mathbf{H}_{pq}^{e,o}(k+1) = \mathbf{H}_{pq}^{e,o}(k) + \mu \text{FFT}[\nabla_{pq}^{e,o}(k); \mathbf{O}_L]^{\text{T}}, \tag{17}$$

where μ is the step-size parameter and the gradient vector $\nabla_{pq}^{e,o}(k)$ is augmented with L zeros.

Equations (16) and (17) place a constraint on the gradient vector, which ensures that frequency-domain tap weights are equivalent to the time-domain counterparts; however, each gradient constraint requires additional FFT and IFFT. Removing the gradient constraint can reduce the complexity of the equalizer as far as the input sequence satisfies some specific conditions; however, by using such unconstraint FDE algorithm, tap-weight vectors do not converge to the Wiener solution as the number of block iterations approaches infinity [16]. Hence, unconstraint FDE is not always reliable.

3. Computational complexity analysis

Considering power consumption and chip space for implementation of the digital signal processing (DSP) algorithm in ASIC or FPGA, we find that the cost for a multiplier is much higher than that for an adder. Hence, in this section, computational complexity is evaluated in terms of the required number of complex multiplications per bit. In the following, the term 'multiplication' always refers to 'complex multiplication'.

We first consider the TDE using the butterfly-structured FIR filters adapted by CMA. The delay spacing is $T/2$ and the tap length is N. To obtain one output symbol from the X port and one output symbol from the Y port of the TDE, we need $8N$ multiplications for output calculations, $4N$ multiplications for tap updating by CMA, and additional 4 multiplications for error-value calculations. By putting these together, the computational complexity C_{TDE} of the adaptive TDE can be expressed as

$$C_{\text{TDE}} = \frac{6N+2}{\log_2(M)}, \tag{18}$$

where M is the number of constellation points on the signal constellation.

#145673 - $15.00 USD Received 11 Apr 2011; revised 20 May 2011; accepted 10 Jun 2011; published 17 Jun 2011

On the other hand, to obtain $N/2$ output symbols from the X port and $N/2$ output symbols from the Y port through processing of one block in our proposed FDE, we need $4N$ multiplications for output calculations of one block, $4N$ multiplications for tap updating by CMA, $2N$ multiplications for error-value calculations, and $12N\log_2(N)$ multiplications for 24 FFT/IFFT processes, which include 4 FFT for inputs, 2 IFFT for outputs, 2 FFT for error-vector calculations, and 16 FFT/IFFT for employing gradient constraint of eight sub-equalizers. For FFT implementation, we assume the use of the classical radix-2 algorithm, which requires $N\log_2(N)/2$ multiplications to execute FFT of N complex numbers [7]. Thus, the computational complexity C_{FDE} of the proposed FDE can be expressed as

$$C_{\mathrm{FDE}} = \frac{12\log_2(N)+10}{\log_2(M)}. \tag{19}$$

Table 1 shows the comparison of computational complexity between FDE and TDE, where we assume the QPSK modulation format (M = 4). From Table 1, it is clear that the proposed adaptive FDE provides much lower complexity than the adaptive TDE when N is 16 or more. This benefit enhances significantly with the increased number of N.

Table 1. Computational Complexity of the Proposed FDE and the Conventional TDE Using FIR Filters Adapted by CMA When Use the Dual-Polarization QPSK Modulation Format

N	**4**	**8**	**16**	**32**	**64**	**128**	**256**
C_{TDE}	13	25	49	97	193	385	769
C_{FDE}	17	23	29	35	41	47	53

4. Experimental verification of the principle of operation of our scheme

In order to verify the principle of operation of our proposed equalizer, we conduct 40-Gbits/s dual-polarization QPSK transmission experiments employing a digital coherent receiver as shown in Fig. 2. The transmitter laser was a distributed-feedback laser diode (DFB-LD) having a center wavelength of 1552 nm and a 3-dB linewidth of 150 kHz. A 20-Gbit/s NRZ-QPSK signal was generated using a $LiNbO_3$ optical IQ modulator (IQM) from two streams of precoded data from an arbitrary waveform generator (AWG) with 2^9-1 pseudo-random binary sequences (PRBS). A 40-Gbit/s dual-polarization signal was then produced with a combination of a polarization-beam splitter (PBS), a fiber delay for pattern decorrelation, and a polarization-beam combiner (PBC). PDL was generated by attenuating one polarization component using a variable optical attenuator (VOA). Then, the signal passed through a commercial PMD emulator (PMDE) and a 100-km-long standard single-mode fiber (SMF). In front of the receiver, a VOA was used to control the received average power. After that, the signal was pre-amplified by an erbium-doped fiber amplifier (EDFA) and detected by a phase-and-polarization diversity coherent optical receiver having a local oscillator (LO) whose characteristics are the same as those of the transmitting laser. The frequency mismatch between the transmitting laser and LO was set below 10 MHz. Outputs from the receiver were sampled at 20 Gsample/s with ADCs, and digitized signals $u_{x,y}(n)$ including 2×10^5 samples were stored for offline DSP.

In the DSP circuit, sampling-phase adjustment, polarization demultiplexing, and signal equalization were done simultaneously either by the proposed FDE or by the conventional TDE, where CMA adapted filter-tap weights. In both cases, the singularity problem inherent in CMA was handled by introducing the training mode prior to the blind CMA mode [17]. The delay-tap length for the TDE was N = 32 and the block length of each sub-equalizer for the FDE was $N/2$ = 16. The step-size parameter was 2^{-10}. Then, the carrier recovery was done by the 4-th power algorithm [18] and the symbols were decoded to estimate the BER. To evaluate the performance of the proposed scheme, we set a mixed channel distortion of 1600-

#145673 - $15.00 USD Received 11 Apr 2011; revised 20 May 2011; accepted 10 Jun 2011; published 17 Jun 2011

ps/nm GVD, 20-ps differential group delay (DGD), and 3-dB PDL and measured BER characteristics for 10^5 symbols per polarization.

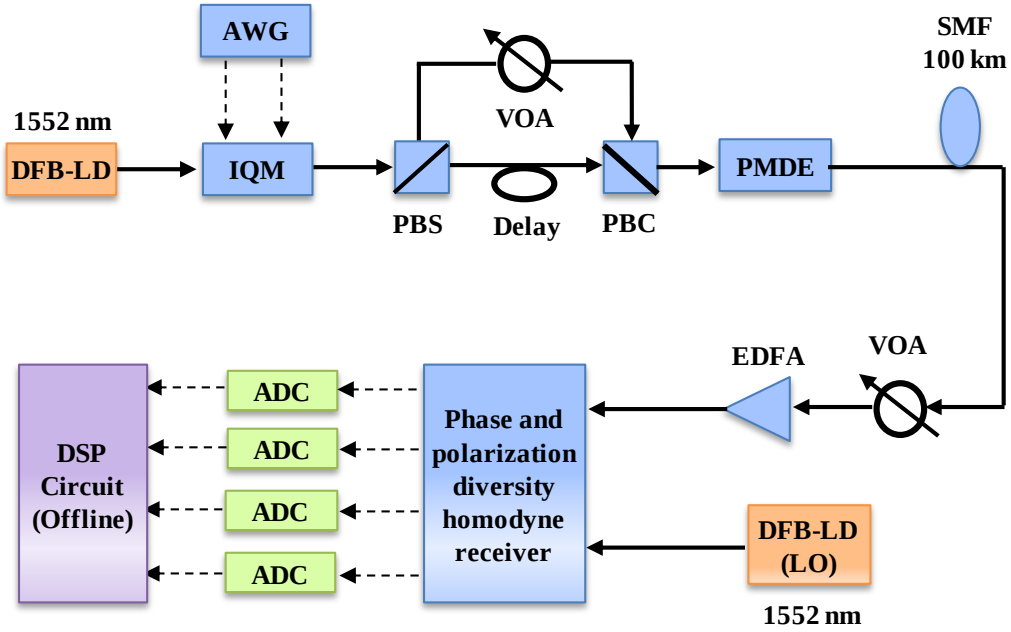

Fig. 2. Schematics of the 40-Gbit/s QPSK transmission system for verifications of the proposed adaptive FDE.

As shown in Fig. 3, the BER performance of the proposed FDE is almost the same as that of the TDE adapted by CMA. The difference in the receiver sensitivity between two polarization tributaries stems from PDL. Thus, we find that the FDE has the same BER characteristics as the TDE, while its computational complexity is lower than that of the TDE as shown in Sec.3

Next, we test the sampling-phase adjustment capability of the proposed adaptive FDE. Receiver outputs were sampled at twice the symbol rate and interpolated to 10 samples per symbol. Such ten-fold oversampled sequences were down-sampled to 2 samples per symbol with different sampling phases and sent to the FDE.

#145673 - $15.00 USD Received 11 Apr 2011; revised 20 May 2011; accepted 10 Jun 2011; published 17 Jun 2011

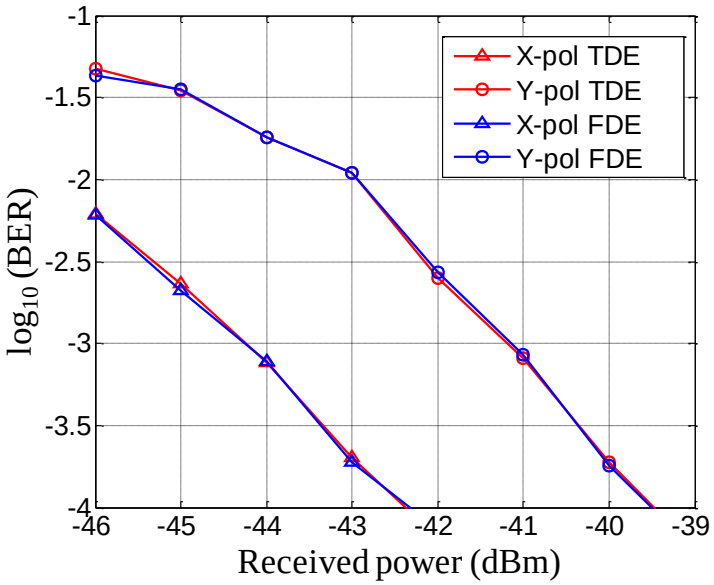

Fig. 3. BER characteristics of the proposed FDE and the conventional TDE adapted by CMA.

Figure 4 shows BER curves for 5 different sampling phases, which are swept with an increment of 10% of the symbol interval. The BER curves are independent of the initial sampling phase, suggesting that the proposed adaptive FDE can adjust the sampling phase optimally in the similar manner to the TDE scheme based on *T*/2-spaced FIR filters [5]. In our experiment, timing jitter may stem from modulation electronics and 100-km fiber transmission. In addition to the static adjustment of the initial sampling phase of ADCs, such relatively-fast timing jitter is also absorbed by the proposed FDE.

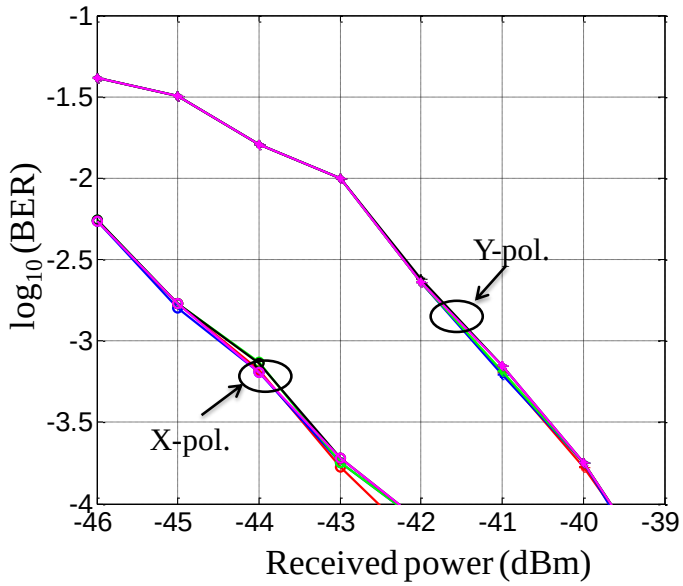

Fig. 4. BER characteristics of the proposed FDE for 5 different sampling phases. These sampling phases are swept with an increment of 10% of the symbol interval.

#145673 - $15.00 USD Received 11 Apr 2011; revised 20 May 2011; accepted 10 Jun 2011; published 17 Jun 2011

5. Conclusion

We have proposed a novel frequency-domain equalizer in digital coherent receivers, which operates on twofold-oversampled input sequences. Such an equalizer performs sampling-phase adjustment of ADCs, polarization demultiplexing, and signal equalization with computational complexity lower than the time-domain equalizer. The DSP circuit can be simplified both by reduction of the number of functional blocks and by lower computational complexity of the equalizer. The satisfactory performance of the proposed equalizer is verified by 40-Gbits/s dual-polarization QPSK transmission experiments.

Acknowledgments

This work was supported in part by Strategic Information and Communications R&D Promotion Programme (SCOPE) (081503001), the Ministry of Internal Affairs and Communications, Japan, and Grant-in-Aid for Scientific Research (A) (22246046), the Ministry of Education, Science, Sports and Culture, Japan.

#145673 - $15.00 USD Received 11 Apr 2011; revised 20 May 2011; accepted 10 Jun 2011; published 17 Jun 2011